

## FACTORS AFFECTING PARTICLE RETENTION IN THERMAL FIELD-FLOW FRACTIONATION

Paul M. Shiundu\*, Stephen M. Munguti and Ben M. Wamalwa

Department of Chemistry, University of Nairobi, P.O. Box 30197, Nairobi, Kenya

(Received October 28, 2001; revised March 22, 2002)

**ABSTRACT.** In this paper, we report a range of factors which affect the retention of colloidal particles in thermal field-flow fractionation (ThFFF). These results are observed among different sizes of polystyrene (PS) latex particles suspended in both aqueous and nonaqueous liquid carriers and very low density lipoproteins in a phosphate buffer. These factors include particle size and chemical composition, field strength, cold-wall temperature of the channel and the nature of the suspension medium. These results show that ThFFF can be used to fractionate colloidal particles according to size and that for an unknown colloidal sample material, a calibration curve must be obtained using particles of similar composition. This is necessary because the degree of retention of the colloidal material is dependent on chemical composition of sample material as evidenced by the chemical composition study. The potential of using ThFFF for physico-chemical characterization of colloidal material is illustrated through the evaluation of thermal diffusion coefficient of PS particles as a function of size, cold-wall temperature, and carrier solution composition. The tunability of the extent of retention of the colloidal particles in a ThFFF channel is illustrated by results of the influence of field strength on retention.

**KEY WORDS:** Factors affecting particle retention, Colloidal particle retention, Thermal field-flow fractionation, Polystyrene latex particles, Lipoproteins

### INTRODUCTION

Field-flow fractionation (FFF) is a separation method introduced by Giddings in 1966 [1]. It is a family of chromatography-like separation techniques applicable to the separation and characterization of macromolecules and particles. Unlike chromatographic separation methods, no stationary phase is used in FFF. In FFF, sample components are subjected to the combined effects of (i) an external field (or gradient) applied perpendicular to the axis of a narrow (50- 250  $\mu\text{m}$  thick) ribbon-like channel structure and (ii) the axial flow of a carrier liquid flowing through the open channel [2]. The velocity profile of the carrier in the channel is approximately parabolic [3], with the higher flow regimes located in the channel centre and the slowest near the walls. Separation of sample components occurs when different sample populations are selectively driven into different flow streamlines by the externally applied field. Species, which are forced to concentrate near the wall due to a strong interaction with the field, will move downstream with relatively slow velocities, thus being retained longer than those species with weaker field interactions. Different fields give different FFF techniques; the best known being sedimentation FFF, thermal FFF, flow FFF, and electrical FFF [2]. These FFF techniques correspond to the "fields" of sedimentation, thermal gradient, cross-flow driving forces, and electrical, respectively.

FFF shows evidence of being a method of extraordinary versatility [4]. Besides its applicability to macromolecules and particles of many different natural and synthetic origins found in both aqueous and nonaqueous media, FFF has shown applicability over an enormous mass range. The experimental range realized to date has a lower extremum of approximately  $10^3$  molecular weight and an upper extremum of about  $10^{18}$  in effective molecular weight, the latter

\*Corresponding author. E-mail: pmsiundu@ics.uonbi.ac.ke

corresponding to a particle of about 100  $\mu\text{m}$  diameter. FFF techniques and applications are described in greater detail elsewhere in the literature [2, 5-12].

Thermal field-flow fractionation (ThFFF) is a technique in which a temperature gradient (as the external “field”) is applied across a channel enclosed between two parallel, highly polished metal bars. Figure 1 shows the general assembly of the ThFFF channel. The channel system used in ThFFF, like that employed for most other FFF methods, has a sandwich construction, the center of which is a thin plastic spacer from which the channel volume has been cut and removed. Copper bars are clamped on either side of this spacer, one to provide heat and the other to remove heat, thereby maintaining a constant temperature drop across the metal bars. The bars are held together by mechanical clamping plates. The temperature drop between the walls,  $\Delta T$ , is controlled by the heat input to the upper bars provided by electrically heated cartridges. This temperature increment provides the driving force necessary for the transport of polymeric and particulate materials across the channel thickness, *i.e.*, induces displacement by thermal diffusion. The phenomenon of thermal diffusion has been known for over a century. The use of this transport process for the fractionation of macromolecules was first reported by Debye and Bueche [13] in 1948.

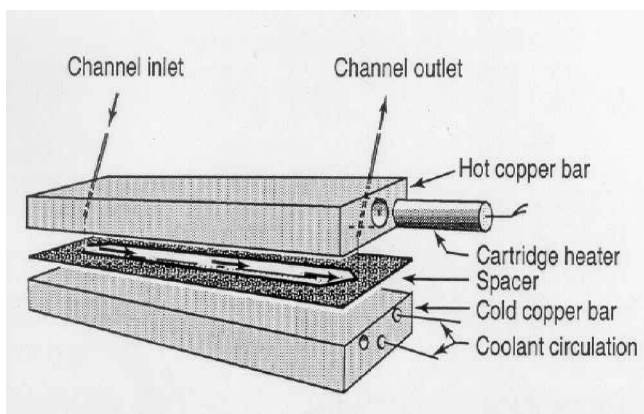


Figure 1. Basic construction of a thermal field-flow fractionation channel.

Thermal field-flow fractionation has traditionally been used for the separation and characterization of polymers with molecular weights ranging from  $10^4$  to  $10^7$  and up [2, 14-18]. The technique has also provided basic thermal diffusion data for polymers [18-20]. In the recent past, however, the applications of ThFFF have been extended to include separation and characterization of particulate materials [21-23] and the technique promises to play a useful role in the fractionation of particles as well as polymers. This is because of the simplicity of the ThFFF operation and a high sensitivity to both particle size and composition; as well as the ready compatibility of the apparatus with both aqueous and nonaqueous carrier solutions which affords the technique greater flexibility than the other FFF techniques.

In this paper, various factors influencing the retention of particles in ThFFF are evaluated. Specific studies reported in this paper include the effects of particle size and composition, temperature drop, cold-wall temperature, and carrier composition on particle retention.

### THEORY OF ThFFF

In ThFFF, the thermal gradient applied across the thin dimension of a narrow ribbon-like channel, forces the sample components toward the cold- (accumulation) wall of the channel due to the phenomenon of thermal diffusion. The resulting build up of concentration is opposed by ordinary diffusion away from the cold-wall. Thus, retention of sample material in ThFFF is controlled by two transport processes: ordinary concentration diffusion coefficient,  $D$ , and thermal diffusion coefficient,  $D_T$  [3]. The  $D_T$  is a basic transport coefficient that describes the movement of matter under an applied temperature gradient. A thin exponential steady-state distribution is soon formed at the wall [14]. Different levels of thermal and ordinary diffusion for different sample component causes these distributions or layers to assume different thicknesses. The distance  $l$  from the accumulation wall to the center of gravity of a particle's distribution "cloud" is related to the transport coefficients of the sample-solvent pair under study by [24, 3]

$$l/l = (D_T/D) dT/dx \quad (1)$$

where  $D_T$  is the thermal diffusion coefficient of the sample-solvent system,  $D$  is ordinary diffusion coefficient of the sample-solvent system, and  $dT/dx$  is the temperature gradient applied across the channel. Multiplying the left hand side and the right hand side of equation 1 by the channel thickness,  $w$  (usually 50 – 250  $\mu\text{m}$ ) yield

$$w/l = (D_T/D) (dT/dx) w = (D_T/D) \Delta T \quad (2)$$

where  $\Delta T$  is the temperature drop between the hot-wall and the cold-wall.

The ratio of  $l$  to  $w$  is dimensionless and is defined as the retention parameter,  $\lambda$ . This is a measure of the extent of interaction between the externally applied field and the sample components. The smaller the  $\lambda$ , the stronger the extent of interaction, and the longer it will take for that sample component to be eluted out of the channel. Hence, from equation 2,

$$\lambda = l/w = (D/D_T) 1/\Delta T \quad (3)$$

The acquisition of a particle size distribution curve for a population of particles is dependent upon establishing a relationship between retention time and particle diameter such that the detector signal generated at any specific time can be identified with the concentration of particles of a specific diameter. Such a relationship can be obtained by a combination of theoretical analysis and calibration procedures as discussed below.

In FFF, retention time  $t_r$  increases monotonically with particle diameter,  $d$ , over a large diameter range. However,  $t_r$  eventually reaches a maximum, after which it begins a long descent with further increases in  $d$ . This reversal in slope of the  $t_r$  versus  $d$  plot constitutes the retention inversion (sometimes referred to as steric inversion). This observation signifies a difference in mechanism of retention for the two sets of population sizes. The mechanism of separation in the (submicron particle diameters) range over which  $t_r$  increases with  $d$  constitutes the normal mode of separation. In this mode of operation, the field-induced velocities with which the sample populations are driven towards the accumulation wall are significantly countered by their ordinary diffusion (since  $D$  is large for particles of smaller diameter). The steric mode of separation applies to the range over which larger particles are retained less than the smaller particle sizes (*i.e.*, order of retention with size is reversed to that of the normal mode).

The retention inversion in FFF provides both difficulties and opportunities in FFF particle characterization. The primary and most obvious difficulty arises from the fact that, successful particle size analysis requires that each retention time element be associated with a specific diameter. Clearly, because of the inversion, each value of  $t_r$  specifies two values of  $d$  and these cannot be distinguished from one another in a single FFF run. This leaves undefined, the question of how much of the detector signal at time  $t_r$  can be attributed to particles of any one of the two diameters as opposed to the other diameter.

One strategy to deal with the double-value problem generated by inversion is to work entirely to the left of the inversion point for small particles and for larger particles, operate on the right side of the inversion maximum. This strategy is given flexibility by virtue of the fact that the inversion diameter (diameter at which order of retention changes) can be shifted up or down by a factor of two or three by changes in the experimental conditions [25].

According to the standard retention theory for normal-mode FFF, the retention time  $t_r$  is related to the dimensionless retention parameter  $\lambda$  of a retained component by the expression [9, 24]

$$t_r/t^o = 1/\{6\lambda [\coth(1/2\lambda) - 2\lambda]\} \quad (4)$$

where  $t^o$  is the void time (the time needed to elute a nonretained component).

For highly retained species in FFF (i.e.,  $\lambda \rightarrow 0$ ), the limiting form of equation 4 becomes [26]

$$t_r/t^o = 1/6\lambda \quad (5)$$

Combining equation 3 and equation 5, we obtain

$$t_r/t^o = D_T \Delta T / 6D \quad (6)$$

From equation 6, it is evident that at constant  $\Delta T$ , variations in  $t_r$  for different particles suspended in the same carrier solution can be attributed to differences in both  $D$  and  $D_T$ .

Using the Stokes-Einstein expression ( $D = kT/3\pi\eta d$ , where  $k$  is the Boltzmann's constant), we can obtain the value of  $D$  for particles of a given  $d$  if the viscosity  $\eta$  of the suspending medium and temperature,  $T$  (in Kelvin) are known. Substituting the Stokes-Einstein expression for  $D$  into equation 6 yields

$$t_r/t^o = \pi\eta d D_T \Delta T / (2kT) \quad (7)$$

which relates the experimentally measured  $t_r$  to particle diameter,  $d$ , and the position-dependent (and therefore temperature-dependent) liquid viscosity  $\eta$  [3].

In order to determine  $d$  at a given  $t_r$ , and thus obtain the particle size distribution (PSD) of a particulate material,  $D_T$  and the temperature-dependent liquid viscosity,  $\eta$  must be known. The position- (or temperature-) dependent viscosity  $\eta$  can be approximated at any point across the channel thickness [3]. However, due to the lack of a sound theoretical basis for  $D_T$ , this term has to be obtained empirically. This uncertainty in the value of  $D_T$  means that a calibration plot with appropriate standards for particles is needed for complete PSD analysis.

Unlike the ordinary diffusion coefficient  $D$ ,  $D_T$  cannot presently be rigorously related to other particle or solvent properties. Therefore, in order that PSD analysis can be achieved without carrying out calibration plots using standard monodispersed particles of the same composition, factors that affect  $D_T$  must be determined; and this is the subject of this study. ThFFF provides a convenient tool to measure  $D_T$ . Rearrangement of equation 7 yields an expression for  $D_T$  as shown below

$$D_T = (2k/\pi d \Delta T) (1/\eta) (t_r/t_r^o)T \quad (8)$$

From this equation (properly corrected for viscosity dependence on temperature across the channel [3]), values of  $D_T$  can be obtained from the experimentally measurable parameter  $(t_r/t_r^o)$  for a given particle of diameter,  $d$  and cold-wall temperature,  $T_c$  (where  $T$  is assumed to be approximately equal to  $T_c$ ). This illustrates the potential of ThFFF to determine the physicochemical properties of particles.

For highly retained sample components, it can be assumed (to a good degree of approximation) that the absolute temperature  $T$  of equations 7 and 8 is equal to the temperature of the cold-wall ( $T_c$ ). This emanates from the understanding that highly retained sample components are pushed closer to the accumulation wall.

For the steric mode of operation, the equivalent retention time expression is [27]

$$t_r/t_r^o = w/(3\gamma d) \quad (9)$$

where  $\gamma$  is the dimensionless steric correction factor, generally of order of unity [27].

## EXPERIMENTAL

The ThFFF system employed in this study is similar in design to the Model T100 polymer fractionator from the FFFractionation (Salt Lake City, Utah, USA). Details of its configuration are provided elsewhere [21]. The mylar channel spacer was confined between two highly polished chrome-plated copper bars. The spacer had a breadth of 2.0 cm, a tip-to-tip length of 46 cm, and a thickness of 76  $\mu\text{m}$ . The top copper bar was electrically heated using cartridges controlled by a variable voltage controller. The cold-wall was cooled using continuously flowing tap water. The temperatures of the hot and cold-walls were monitored through four thermal sensors that were inserted (two in each wall) into wells drilled into both the top and bottom bars. The  $\Delta T$  and cold-wall temperature values used for each experimental study are provided in the figure captions. Aqueous carrier liquid was used in this study (unless stated otherwise). This was delivered using a Model M-6000A pump from Waters Associates (Milford, MA, USA). The ionic strength (where applicable) of the aqueous solutions was modified using tetrabutyl ammonium perchlorate (TBAP) or sodium azide (which also served as a bactericide). In some cases, the aqueous carriers contained 0.1% FL-70 surfactant; otherwise, double distilled water was used in all cases. The flow-rate used was 0.30 mL/min (unless stated otherwise). A Model UV-106 detector from Cole Scientific (Calabasas, CA, USA) operating at 254 nm wavelength was used to detect particles eluting from the ThFFF channel. The hard copy of the detector signal was recorded using an OmniScribe chart recorder from Houston Instruments (Austin, TX, USA). Samples were injected via a 20  $\mu\text{L}$  loop injection valve.

Standard polystyrene (PS) latex particles of different sizes used in this study were obtained from Duke Scientific (Palo Alto, CA, USA).

## RESULTS AND DISCUSSION

The development of ThFFF as a viable technique for particle size analysis is dependent upon our understanding of all the factors that influence particle retention. This is important considering the fact that the phenomenon responsible for the driving force, thermal diffusion, is both complex and poorly understood [2]. This has necessitated the use of ThFFF itself to build empirical evidence on the relationship of thermal diffusion to analytically relevant parameters such as particle size, chemical composition, solvent composition, field-strength, cold-wall temperature, and surface composition.

In the sections that follow, experimental evidence is provided on the factors, so far, established, that affect particle retention in ThFFF. Attempts are made to correlate the experimental observation with the theoretical expressions given earlier in this manuscript.

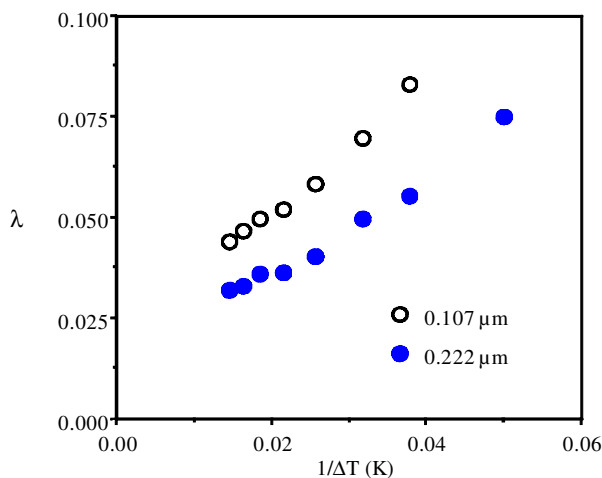


Figure 2. Plots of retention parameter  $\lambda$  versus  $1/\Delta T$  for two diameters of polystyrene latex particles suspended in an aqueous carrier liquid. Experimental conditions: flow rate = 0.30 mL/min, and concentration of TBAP = 0.01 mM.

According to equation 3, the retention parameter  $\lambda$  should have a linear dependence on  $1/\Delta T$  if the ratio of  $D$  to  $D_T$  is independent of the temperature drop between the hot- and cold-walls,  $\Delta T$ , and in the absence of any perturbations of the normal particle retention induced by the thermal field. Figure 2 shows a plot of  $\lambda$  (retention parameter) versus the reciprocal of  $\Delta T$  for two standard polystyrene (PS) particle sizes of 0.107 and 0.222  $\mu\text{m}$  suspended in an aqueous carrier liquid. The concentration of TBAP used was 0.01 mM in order to modify the ionic strength of the carrier; the importance of which has been established and reported elsewhere [22]. From this figure, it is evident that for both particle sizes, larger values of  $\Delta T$  (*i.e.*, small values of  $1/\Delta T$ ) causes increased interaction between the externally applied field (*i.e.*, smaller values of  $\lambda$ ) and the sample components. This is significant because of the tunability of the retention time by appropriately adjusting the applied  $\Delta T$ . Also of particular significance is the linearity in the relationship between  $\lambda$  and  $1/\Delta T$  for the relatively lower  $\Delta T$  (*i.e.*, larger  $1/\Delta T$ )

values. Deviations from linearity that is witnessed for larger values of  $\Delta T$  (*i.e.*, lower  $1/\Delta T$ ) may be attributed to increased perturbations on the particle retention due to increased particle-wall electrostatic interactions as the particles approach the accumulation wall more closely. It is possible that the 0.01 mM TBAP salt concentration employed is not sufficient to eliminate these perturbations. Further studies are being conducted to establish this. Figure 2 therefore, illustrates the influence that the field strength has on particle retention.

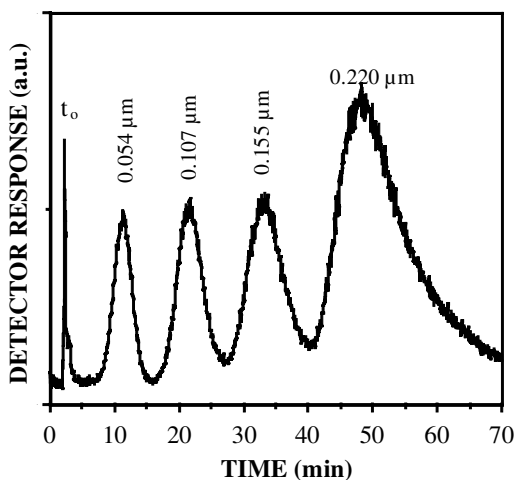


Figure 3a. Separation of submicron polystyrene latex particles suspended in an aqueous medium. Experimental conditions: concentration of TBAP = 1.0 mM, flow rate = 0.30 mL/min, and  $\Delta T = 24$  K.

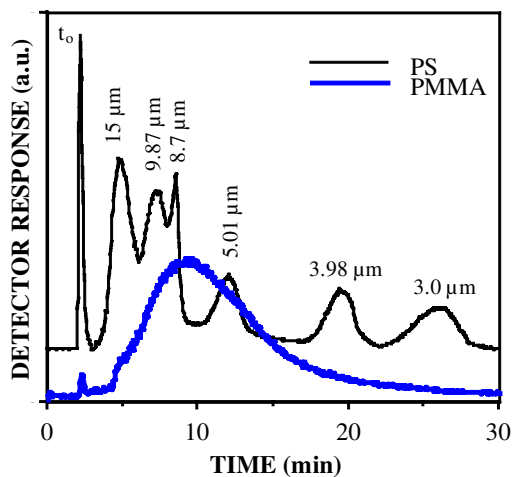


Figure 3b. Superimposed elution profiles of standard micron size polystyrene latex particles (light-solid line) and polydispersed PS sample matrix (thick-solid line) suspended in

aqueous solution. Experimental conditions: concentration of TBAP = 1.0 mM, flow rate = 0.30 mL/min, and  $\Delta T = 24$  K.

Figure 3a shows the ability of ThFFF to fractionate submicron PS particles suspended in an aqueous carrier medium according to particle size. The concentration of TBAP used was 1.0 mM and the  $\Delta T$  was 24 K. These results are in agreement with equation 7, in which particle retention time,  $t_r$ , is proportional to particle size,  $d$  in the “normal” mode of operation. Hence, particle retention is a function of particle size among other parameters. In the steric mode of operation, however, the order of particle retention is reversed to that observed in the normal mode of operation as expressed in equation 9. Figure 3b shows superimposed elution profiles: one (single line) for separation of a mixture of standard micron sized PS latex particles; and the second, a fractogram of a polydisperse PS sample matrix. This figure too, shows that ThFFF can be used to fractionate micron size particles as a function of size. However, for micron size particles, larger-size particles elute earlier than smaller size particles (*i.e.*, steric mode). It must be stated here that, retention times of standard particle samples can only be used as a calibration for an unknown sample population, only if the two sets have the same chemical composition (see later for clarification).

The temperature term  $T$  of equation 7 refers to the temperature of the equilibrium position that the sample component is located. For highly retained components, this temperature can be equated to the temperature of the cold-wall ( $T_c$ ). According to the Stokes-Einstein expression (where  $D = kT/3\pi\eta d$ ), an increase in temperature,  $T$  (which is approximated to be equal to the cold-wall temperature,  $T_c$  for well retained particles) implies a larger value of  $D$ ; which translates to a smaller value of the  $t_r/t'_0$  ratio according to equation 6. Previous studies involving PS latex particles in several nonaqueous suspensions [22] have produced results that are consistent with this theory. However, results of Figure 4 show that PS particles suspended in an aqueous medium have a linear dependency between  $t_r/t'_0$  and  $T_c$ , with the slope of the plots increasing with particle size. These observations are consistent with the conclusion that  $D_T$  is dependent on both  $T_c$  and the composition of the suspending medium. Otherwise, plots of  $t_r/t'_0$  versus  $1/T_c$  should be linear. This calls for further experiments to establish the exact nature of the dependence of  $D_T$  on  $T_c$  and composition. The experiments of Figure 4 were carried out using an aqueous solution containing 0.1% FL-70 surfactant and 0.02% sodium azide (functioning both as a bactericide and for ionic strength modification) at a  $\Delta T$  of 30 K.

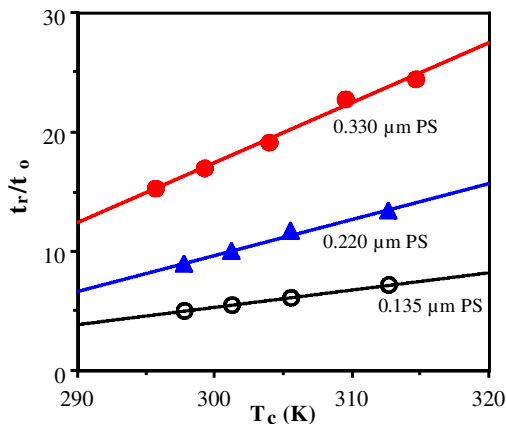
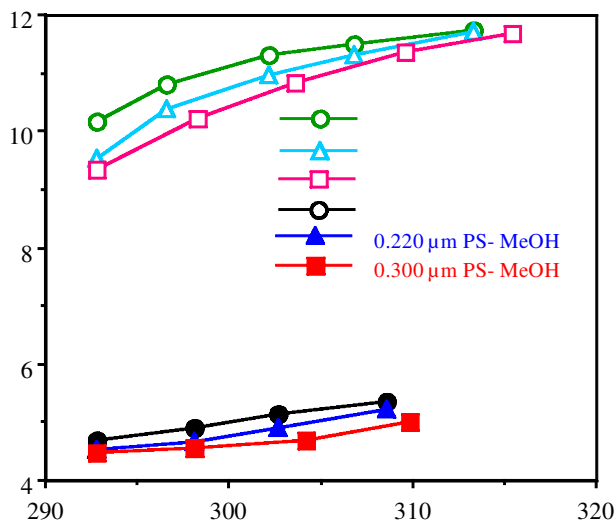


Figure 4. Plots of  $t_r/t_o$  versus cold-wall temperature for three PS latex particles in an aqueous carrier liquid comprising of 0.1% FL-70 surfactant and 0.02% sodium azide. The flow rate = 0.30 mL/min, and the  $\Delta T = 30$  K.

Evaluation of the values of  $D_T$  for different sizes of PS latex particles suspended in acetonitrile (ACN) and methanol (MeOH) carrier solutions (the ionic strengths of both media adjusted using 1.0 mM concentration of TBAP) was carried out using equation 8 (software for analysis and based on the temperature/viscosity correction [3] was obtained from the Field-Flow Fractionation Research Center, University of Utah, Salt Lake City, Utah – USA). The results of the study are shown in Figure 5 and they confirm the dependency of  $D_T$  on  $T_c$  for three different sizes of PS latex particles suspended in the nonaqueous carrier liquids. The experiments were conducted using a flow-rate of 0.30 mL/min and a  $\Delta T$  of 55 K. Another notable observation from these plots is the difference in the magnitude of  $D_T$  for the PS particles between the two carrier suspensions.  $D_T$  values are much lower in methanol than in acetonitrile. This suggests that particle retention in ThFFF is not only a function of particle size but also of the composition of the carrier media. This dependence is not only evident among different types of nonaqueous suspensions (*e.g.*, acetonitrile and methanol) but also in aqueous carrier liquids [21-23].



(*i.e.*, VLDL and PS). The order of retention for the PS particles is however, consistent with expectation.

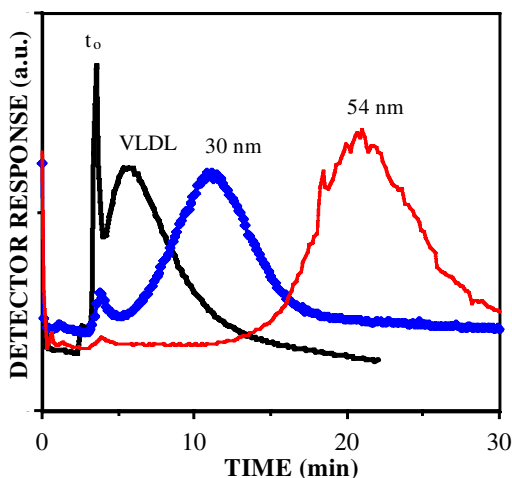


Figure 6. Superimposed elution profiles of very low-density lipoproteins (VLDL) of nominal hydrodynamic diameter of 55 nm, 30 nm PS and 54 nm PS latex particles. Experimental conditions: phosphate buffer flowing at 0.20 mL/min and  $\Delta T = 40$  K.

## CONCLUSIONS

In this paper, we demonstrate the ability of ThFFF to fractionate particulate matter according to size, both in the normal mode (for submicron size particles) and steric (for micron size particles) modes of operation. It is also evident that the degree of particle retention in ThFFF is influenced by a number of other factors which affect the thermal diffusion coefficient; the driving force behind retention. Among these factors include, chemical composition of the sample and the suspension medium, ionic strength of the medium, field strength, and the cold-wall temperature. Whereas the retention dependence on the chemical composition of the particulates may be viewed as a disadvantage, since only standard particles of similar composition as the unknown must be used for calibration, the prospect of fractionating colloidal materials according to their composition is significant.

In order that ThFFF can be effectively used as a tool for separation and physico-chemical characterization of particulate or colloidal sample materials, it is necessary that all the factors influencing retention be identified and their influence on the thermal diffusion coefficient be well understood. This study, in part, identifies factors that influence  $D_T$ , and is by no means exhaustive. A great deal more work is needed to define and exploit these factors.

## ACKNOWLEDGMENT

This work was supported in part by Grant No. 96-116RG/CHE/AF/AC from the Third World Academy of Sciences (TWAS) Research Grants Scheme. S.M.M. acknowledges support from

the German Academic Exchange Services (DAAD) for the award of a scholarship in support of his graduate school program.

## REFERENCES

1. Giddings, J.C. *Sep. Sci.* **1966**, 1, 123.
2. Giddings, J.C. *Science* **1993**, 260, 1456.
3. Gunderson, J.J.; Caldwell, K.D.; Giddings, J.C. *Sep. Sci. Technol.* **1984**, 19, 667.
4. Giddings, J.C. *Anal. Chem.* **1981**, 53, 1170.
5. Ratanathanawongs, S.K.; Giddings, J.C. *Chromatography of Polymers: Characterization by SEC and FFF*, Provder, T. (Ed.); ACS Symp. Ser. No. 521, American Chemical Society: Washington, D.C.; **1993**; p 13.
6. Martin, M.; Williams, P.S. *Theoretical Advancement in Chromatography and Related Techniques*, Dondi, F.; Guiochon, G. (Eds.); Vol. 383, NATO ASI Series C: Mathematical and Physical Sciences, Kluwer: Dordrecht; **1992**; p. 513.
7. Beckett, R.; Hotchin, D.M.; Hart, B.T. *J. Chromatogr.* **1990**, 517, 435.
8. Caldwell, K.D. *Anal. Chem.* **1988**, 60, 959A.
9. Giddings, J.C. *Chem. Eng. News* **1988**, 66, 34.
10. Giddings, J.C.; Caldwell, K.D. in *Physical Methods of Chemistry*, Rossiter, B.W.; Hamilton, B.W. (Eds.); Vol. 3B, Wiley: New York; **1989**; p 867.
11. Yau, W.W.; Kirkland, J.J. *Sep. Sci. Technol.* **1981**, 16, 577.
12. Giddings, J.C. *Pure Appl. Chem.* **1979**, 51, 1459.
13. Debye, P.; Bueche, A.M. in *High Polymer Physics*, Chemical Publishing Co: New York; **1948**.
14. Giddings, J.C. in *Unified Separation Science*, Wiley: New York; **1991**.
15. Gunderson, J.J.; Giddings, J.C. *Anal. Chim. Acta* **1986**, 189, 1.
16. van Asten, A.C.; Venema, E.; Kok, W. Th.; Poppe, H. *J. Chromatogr.* **1993**, 644, 83.
17. Kirkland, J.J.; Rementer, S.W. *Anal. Chem.* **1992**, 64, 904.
18. Schimpf, M.E. *J. Chromatogr.* **1990**, 517, 405.
19. Schimpf, M.E.; Giddings, J.C. *J. Polym. Sci.: Polym. Phys. Ed.* **1989**, 27, 1317.
20. Schimpf, M.E.; Giddings, J.C. *J. Polym. Sci.: Polym. Phys. Ed.* **1990**, 28, 2673.
21. Liu, G.; Giddings, J.C. *Chromatographia* **1992**, 34, 483.
22. Shiundu, P.M.; Liu, G.; Giddings, J.C. *Anal. Chem.* **1995**, 67, 2705.
23. Shiundu, P.M.; Giddings, J.C. *J. Chromatogr. A* **1995**, 715, 117.
24. Giddings, J.C. *Sep. Sci. Technol.* **1984**, 19, 831.
25. Myers, M.N.; Giddings, J.C. *Anal. Chem.* **1982**, 54, 2284.
26. Giddings, J.C.; Williams, P.S.; Beckett, R. *Anal. Chem.* **1987**, 59, 28.
27. Giddings, J.C. *Analyst* **1993**, 118, 1487.